Title

Relative influence of precession and obliquity in the early Holocene: Topographic modulation of subtropical seasonality during the Asian summer monsoon

Authors

Wu, Chi-Hua
Lee, Shih-Yu
Chiang, John CH

Publication Date

2018-07-01

DOI

10.1016/j.quascirev.2018.05.021

Peer reviewed

Relative influence of precession and obliquity in the early Holocene: Topographic modulation of subtropical seasonality during the Asian summer monsoon

Chi-Hua Wu[a] Shih-Yu Lee[a] John C.H. Chiang[b]

[a]Research Center for Environmental Changes, Academia Sinica, Taipei, Taiwan, ROC

[b]Department of Geography and Berkeley Atmospheric Sciences Center, University of California, Berkeley, CA, USA

Abstract

On orbital timescales, higher summer insolation is thought to strengthen the continental monsoon while weakening the maritime monsoon in the Northern hemisphere. Through simulations using the Community Earth System Model, we evaluated the relative influence of perihelion precession and high obliquity in the early Holocene during the Asian summer monsoon. The major finding was that precession dominates the atmospheric heating change over the Tibetan Plateau–Himalayas and Maritime Continent, whereas obliquity is responsible for the heating change over the equatorial Indian Ocean. Thus, precession and obliquity can play contrasting roles in driving the monsoons on orbital timescales.

In late spring–early summer, interior Asian continental heating drives the South and East Asian monsoons. The broad-scale monsoonal circulation further expands zonally in July–August, corresponding to the development of summer monsoons in West Africa and the subtropical Western North Pacific (WNP) as well as a sizable increase in convection over the equatorial Indian Ocean. Tropical and oceanic heating becomes crucial in late summer. Over South Asia–Indian Ocean (50°E−110°E), the precession maximum intensifies the monsoonal Hadley cell (heating with an inland/highland origin), which is opposite to the meridional circulation change induced by high obliquity (heating with a tropical origin). The existence of the Tibetan Plateau–Himalayas intensifies the precessional impact. During the late-summer phase of the monsoon season, the effect of obliquity on tropical heating can be substantial. In addition to competing with Asian continental heating, obliquity-enhanced heating over the equatorial Indian Ocean also has a Walker-type circulation impact, resulting in suppression of precession-enhanced heating over the Maritime Continent.

1. Introduction

Paleoclimate data provide insights to understanding extreme changes in the characteristics of global monsoons (An et al., 2015; Caley et al., 2011; Cheng et al., 2012; Chiang et al., 2015; Mohtadi et al., 2016). A model-data comparison is useful to test existing hypotheses (Cai et al., 2017; Caley et al., 2014; Dallmeyer et al., 2013; Dayem et al., 2010; Jin et al., 2014), including the direct monsoonal response to orbital forcing and a further

modulation due to oceanic feedback and topographic effect (Kutzbach et al., 2008; Liu et al., 2003, 2004, 2015; Shi et al., 2011, 2012). On Milankovitch timescales, an increase in summer insolation is thought to strengthen and shift the northern hemisphere summer monsoons over land (Battisti et al., 2014; Wang et al., 2016; Wu et al., 2016a). However, the relative contribution of major orbital parameters (precession and obliquity) is still not adequately understood (Bosmans et al., 2015; Lee and Poulsen, 2009; Wu et al., 2016b). As was shown in this study, the impacts of precession and obliquity on enhancement of tropical convection can be separately identified, in terms of their influence on the topographic driving of climate and the seasonal dependence of changes. Traditional assumptions, that precession dominates in the tropics and obliquity primarily alters meridional thermal gradients (Mantsis et al., 2014; Merlis et al., 2013; Mohtadi et al., 2016), warrant further examination.

The summer monsoon circulation over the Asian continent can be explained using the Sverdrup vorticity balance, with lower-tropospheric cyclonic and upper-tropospheric anticyclonic circulations being accompanied by ascending southerly flow in the east and descending northerly flow in the west (Duan and Wu, 2005; Rodwell and Hoskins, 2001; Wu et al., 2009b). The ascending southerly flow bordering the Western North Pacific (WNP) subtropical high is crucial for the East Asian Meiyu–Baiu system. To the west, the descending northerly flow – which is also associated with the monsoon–desert mechanism (Rodwell and Hoskins, 1996, 2001) – strongly influences the monsoon break in India (Choudhury and Krishnan, 2011) and the monsoon inversion over the Arabian Sea (Wu et al., 2017a). Changes in large-scale subtropical circulation alter the behavior of the embedded summer monsoons across West Africa, Asia, and the subtropical WNP.

Studies have firmly established that in the early Holocene, the summer monsoons in Africa (Rachmayani et al., 2015; Tuenter et al., 2003) and East and South Asia (An, 2000; Dallmeyer et al., 2010; Fleitmann et al., 2007) were stronger and shifted northward compared with at present, whereas the WNP monsoon trough was nearly absent (Wu et al., 2016a). Additionally, the enhanced convection in the Maritime Continent and equatorial Indian Ocean has been partly attributed to the suppression of convection in South Asia between 10°N and 20°N and the strengthening of the WNP subtropical high (Wu et al., 2016a). One proposed early Holocene paradigm is that the continental monsoon was more intense, whereas the maritime monsoon was nonexistent. Limited studies have emphasized the orbital-induced changes in seasonality among the distinct northern hemisphere summer monsoons (Braconnot and Marti, 2003; Braconnot et al., 2008). In the early Holocene, with summer solstice occurring near perihelion, insolation was higher than at present and this was reported to have a larger impact on the South Asian monsoon than on the African summer monsoon, whereas in the Eemian, when increased summer insolation occurred in late summer, the African summer monsoon was more strongly influenced (Braconnot et al., 2008).

Further modeling results suggested that the South Asian monsoon is most sensitive to spring-to-early-summer insolation, whereas the African monsoon is most sensitive to summer insolation (Rachmayani et al., 2016).

In Asia, topographic driving of seasonal details is dramatic. Associated with an increase in Tibetan Plateau heating in spring and early summer, the present-day South Asian summer monsoon and Meiyu–Baiu reach a mature stage in mid-June, which maintains the subtropical anticyclone in the upper troposphere until late July when the upper-tropospheric anticyclone expands sideways. The evolution across late July coincides with the development of the monsoons in West Africa and the subtropical WNP as well as convection over the equatorial Indian Ocean (Wu et al., 2017a). In this regard, an orbital-scale change in the subtropical circulation and monsoon systems may still be dependent on seasons and subseasons and be topographically regulated.

Recent modeling results have suggested that both perihelion precession and high obliquity had substantial effects on the early Holocene Asian summer monsoon changes (Wu et al., 2016a, 2016b); the changes in the South Asian and North Pacific highs as well as the monsoon–midlatitude interaction are arguably related to the obliquity-induced meridional gradients of geopotential height and temperature. Following previous investigations in model-data comparison, this study aimed to understand the relative effect of precession and obliquity on the Asian monsoon seasonality, from a regional to a broad scale. We also explored the potential connection between the orbital-induced heating changes with inland and highland origins (Tibetan Plateau–Himalayas) and those with a tropical origin because the Asian summer monsoon is topographically dependent (Kitoh, 2002; Tada et al., 2016; Wu et al., 2018; Wu and Hsu, 2016). The paper is organized as follows. Section 2summarizes the paleoclimatic proxy records during the past few precession and obliquity cycles and introduces the model and experimental design. Section 3 highlights the summer monsoon response to the early Holocene orbital change. Section 4 investigates the relative roles of precession and obliquity in modulating the early Holocene summer monsoon. Section 5explores the topographic effects on modulating orbital forcing. The discussion and conclusions are provided in Section 6.

2. Proxy data, model, and experimental design

2.1. Paleoclimatic proxy records

We first attempted to characterize regional differences in paleoclimatic changes during the past few precession and obliquity cycles (150 ka BP to the present day, Fig. 1) by collecting together 10 proxy records for South Asia, the Indian Ocean, and the Maritime Continent (Table 1). Proxy data included cave and marine core oxygen isotopes (Carolin et al., 2016; Jung et al., 2009; Kathayat et al., 2016; Mohtadi et al., 2010; Stott et al., 2002; Yuan et al., 2004) and planktonic foraminiferal Mg/Ca (Anderson and Prell, 1993; Gibbons et al., 2014; Saraswat et al., 2005, 2013) downloaded

from the paleoclimatology data website of the National Oceanic and Atmospheric Administration (NOAA) (https://www.ncdc.noaa.gov/data-access/paleoclimatology-data). As demonstrated by the reconstruction in Borneo, higher insolation considerably depletes oxygen isotopes (Fig. 1a and b). Consistent with previous studies, our comparison suggested that the tropical records exhibit essential precessional power in phase with low-latitude summer insolation. When high obliquity and a precession minimum overlapped (e.g., 20–5 ka BP and 135–120 ka BP) (Fig. 1a), the available proxy records suggest a warming or wetting trend in the tropical region(equatorial Indian Ocean, Indo-Pacific warm pool, and Borneo, Fig. 1b) and inland South Asia (Bittoo and Dongge caves) as well as a cooling trend in the subtropical region (Oman) (Fig. 1c–f). These results illustrated the influence of insolation and climatic trends when two orbital parameters were out of phase; however, the individual contributions of precession and obliquity are unclear.

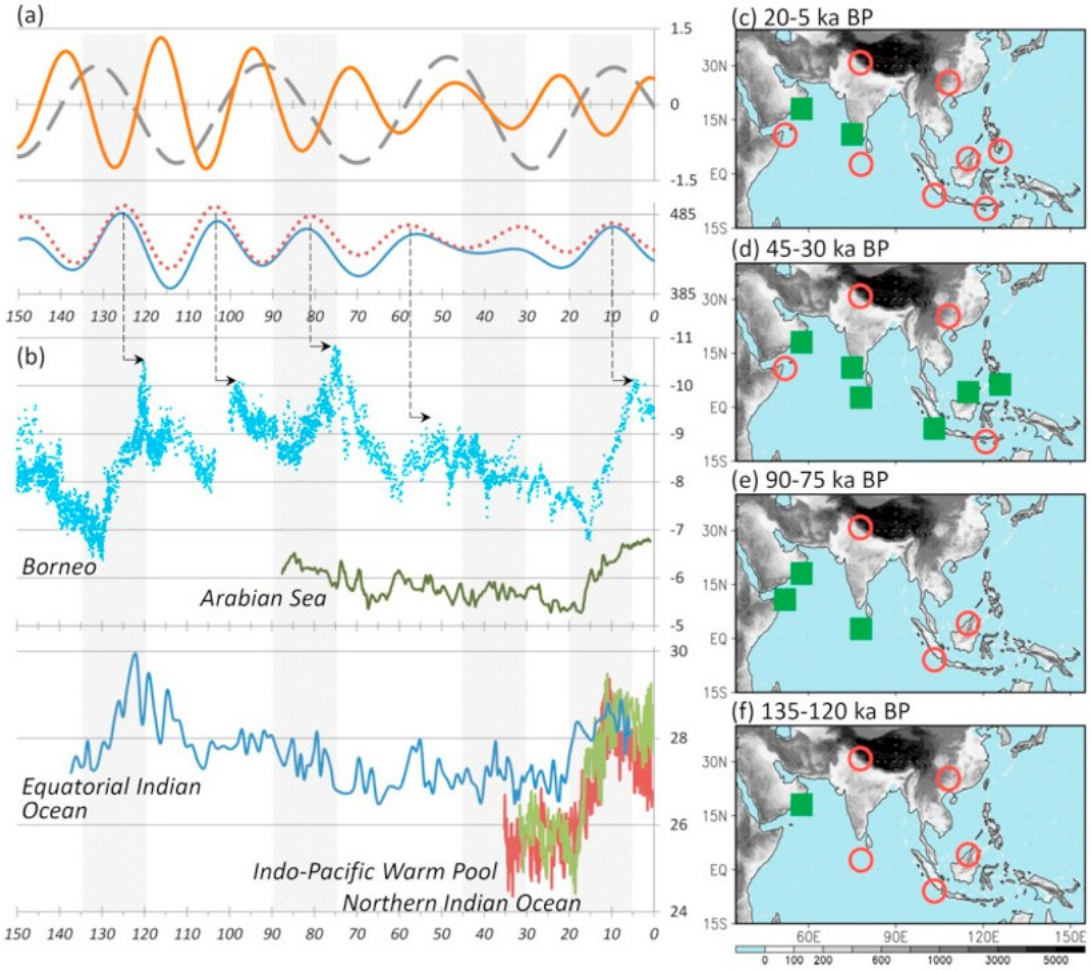

Fig. 1. (a) Evolution over 150 ka BP to the present of orbital parameters (precessional index × 30: solid-orange line; obliquity minus 23.5°: gray-dashed line) and insolation at 15°N (red dotted line) and at 65°N in July (solid blue line). (b) Paleoclimate proxy records for Borneo, the Arabian Sea, the equatorial Indian Ocean, the Indo-Pacific warm pool, and the northern Indian Ocean (see Table 1 for details). Trends in all the proxy records listed in Table 1 during 20–5 ka BP, 45–30 ka BP, 90–75 ka BP, and 135–

120 ka BP (c–f). Red circles (green boxes) denote an increasing (decreasing) trend, corresponding to cold-to-warm or dry-to-wet (warm-to-cold or wet-to-dry) changes. Gray shading denotes the topography (unit: m).

Table 1. Geographic locations, parameters, data length, and references of the paleoclimate proxy records used in this study.

Location	Longitude(°E)	Latitude (°N)	Parameter	Period relative to 1950 (ka BP)	Reference
India	77.78	30.79	oxygen isotopes	283.817–0.874	Kathayat et al. (2016); Bittoo Cave
Eastern China	108.08	25.28	oxygen isotopes	163.500–0.116	Yuan et al. (2004); Dongge Cave
Borneo	114.83	4.15	oxygen isotopes	161.533 ~ −0.055	Carolin et al. (2016)
Pacific Warm Pool	125.83	6.30	oxygen isotopes	67.592–0	Stott et al. (2002); MD98-2181
Eastern Tropica	103.25	−5.94	oxygen isotopes	131.400–0	Mohtadi et al. (2010)

Location	Longitude(°E)	Latitude (°N)	Parameter	Period relative to 1950 (ka BP)	Reference
l Indian Ocean					
Arabian Sea	51.95	10.77	oxygen isotopes	87.582–0.956	Jung et al. (2009); NIOP905
Oman	57.61	18.05	Foraminifera (forams/gram)	300.000–0	Anderson and Prell (1993); Upwelling
Northern Indian Ocean	75.00	10.98	sea surface temperature	31.600–0.120	Saraswat et al. (2013)
Equatorial Indian Ocean	78.00	2.67	sea surface temperature	137.333–6.250	Saraswat et al. (2005); Foraminiferal Mg/Ca
Indo-Pacific Warm	120.92	−9.59	sea surface temperat	35.240–0.025	Gibbons et al. (2014);

Location	Longitude(°E)	Latitude (°N)	Parameter	Period relative to 1950 (ka BP)	Reference
Pool			ure		Foraminiferal Mg/Ca

We also examined climatic trends when obliquity was decreasing around a precession minimum over 150 ka BP to the present. It was found that a sharp decrease in obliquity may have substantially affected the proxy records over the equatorial Indian Ocean. During 90–75 ka BP, when a precession was at a minimum and obliquity was decreasing, the proxy records show a change that was opposite to that during 20–5 ka BP and 135–120 ka BP (compare Fig. 1e with Fig. 1c–f). The period when the two orbital parameters were in phase inspires further questions. Additionally, a large regional contrast is observable during 45–30 ka BP, when obliquity and precession had identical tendency. When compared with 20–5 ka BP, during which obliquity increased and precession decreased, an opposite change is revealed in the equatorial Indian Ocean and regions surrounding Borneo (compare Fig. 1c with Fig. 1d). This justifies exploring the dynamical cause using a climate model. By doing this, we diagnosed the relative contributions of precession and obliquity in the orbital time scale.

2.2. Model

The Community Atmospheric Model (CAM) Version 5.1 of the National Center for Atmospheric Research (NCAR) coupled with the slab ocean model (SOM) (http://www.cesm.ucar.edu) was used. Parameterizations in the CAM include moist processes (deep or shallow convection and largescale condensation), cloud macrophysics and microphysics and radiation, surface models, and turbulent mixing (planetary boundary layer, vertical diffusion, and gravity wave drag). The CAM/SOM were integrated using a finite volume dynamical core with 30 vertical levels in the CAM at a horizontal resolution of approximately 1°, with the boundary and initial conditions of the simulations being adopted from the Community Earth System Model (CESM) preindustrial control experiment (Vertenstein et al., 2010).

The CAM/SOM framework is advantageous in the sense that we can equilibrate to the forcing a lot faster. For each simulation case, the model was integrated for 40 years and the outputs for the latest 20 years were analyzed. Our simulations and previous studies (Danabasoglu and Gent, 2009; Kitoh, 2002) indicated that 20 years were sufficient for the model to reach a quasi-equilibrium state. We have recognized that the CAM/SOM produced a more realistic climatology of the Asian summer monsoon than did the CAM standalone simulation forced by the prescribed sea surface temperature(figure not shown). However, the CAM/SOM still lacks simulation of important ocean dynamical feedback processes, the most significant for us would be the lack of a tropical Pacific response, since ENSO is known to affect today's Asian monsoon.

2.3. Experimental design

We chose the Holocene climate with a relatively warm state as the baseline climate to perturb. The control simulation had an aphelion precession of 103° and obliquity of 23.4° (hereafter referred to as the PmaxO23 simulation). A simulation with early Holocene orbital conditions was

performed using orbital parameters of 11 ka BP; that is a perihelion precession of 279° and high obliquity of 24.2° (the PminO24 simulation). Other boundary conditions in the PminO24 simulation were kept the same as in the control. To explore the impact of obliquity, a simulation with the same orbital parameters as PminO24 simulation, except for a low obliquity of 22.3°, was performed (the PminO22 simulation). The eccentricity was relatively low in the Pmax (0.0167) and Pmin (0.0195) sets.

To explore the role of the Tibetan Plateau–Himalayas in modulating the monsoonal response to orbital changes, we performed a simulation with a flattened Tibetan Plateau (T0 experiment) by reducing the height of the region centered on the Plateau (45°E−125°E, 20°N–60°N) by 90% but using otherwise the control run orbital parameters. We then conducted “flattened Tibet” simulations with the orbital parameters of PmaxO23, PminO24, and PminO22 (PmaxO23_T0, PminO24_T0, and PminO22_T0, respectively). There were six simulations in total. Each had an integration length of 40 years.

Table 2 summarizes the orbital parameters (eccentricity, precession, and obliquity) and annual mean insolation (in the Northern Hemisphere) of the simulations.

Table 2. Orbital parameters (eccentricity, precession, obliquity) and annual mean northern hemisphere insolation (in May–June and August, W m^{-2}) at the top of the atmosphere in the CAM/SOM experimental simulations. The height of the region centered on the Plateau (45°E−125°E, 20°N–60°N) was reduced by 90% in the T0 experiments.

Experiments	E	P	O	Insolation (May–June)	Insolation (August)
PmaxO23 & PmaxO23_T0	0.0167	103	23.4	449.32	410.65
PminO24 & PminO24_T0	0.0195	279	24.2	480.92	422.20
PminO22 & PminO22_T0	0.0195	279	22.3	471.22	416.70

3. Characteristics of the early Holocene summer monsoon over and surrounding Asia

This section examines the overall difference in atmospheric circulationbetween the PminO24 and PmaxO23 simulations as a prelude to highlighting the relative roles of precession and obliquity and the role of the Plateau. The main focus was on the temporal evolution of the large-scale subtropical circulation and summer monsoon.

3.1. Atmospheric heating differences and Asian summer monsoon subsystems

Strong heating over the Tibetan Plateau is a driving mechanism of the Asian summer monsoon (Wu et al., 2012; Wu and Zhang, 1998; Yanai et al., 1992). In the present climate state (PmaxO23), the magnitude of Tibetan Plateau heating as identified by the atmospheric column-integrated total heating over a 3-km height of the Tibetan Plateau (Hsu and Liu, 2003) increases gradually in May (Fig. 2a), driving the South Asian summer monsoon in mid-to-late May as illustrated by the monsoon Hadley index (Fig. 2b); the monsoon Hadley index was defined by the meridional wind shear between 850 hPa and 200 hPa averaged over the region (70°E−110°E, 10°N–30°N) (Goswami et al., 1999). The arrival of the lower-tropospheric monsoon flow at the southern Tibetan Plateau–Himalayas is positive feedback to the Tibetan Plateau heating in the form of “candle-like heating” (Chen et al., 2014; Wu et al., 2018), which accelerates Tibetan Plateau heating in June. Presently, the peak timings of the Tibetan Plateau heating and monsoon Hadley index coincide in late June (Fig. 2a and b). With
early Holocene insolation(PminO24), the Tibetan Plateau heating and monsoon Hadley index rapidly increase and reach their present-day values earlier in late May, suggesting an earlier effect of the Himalayas.

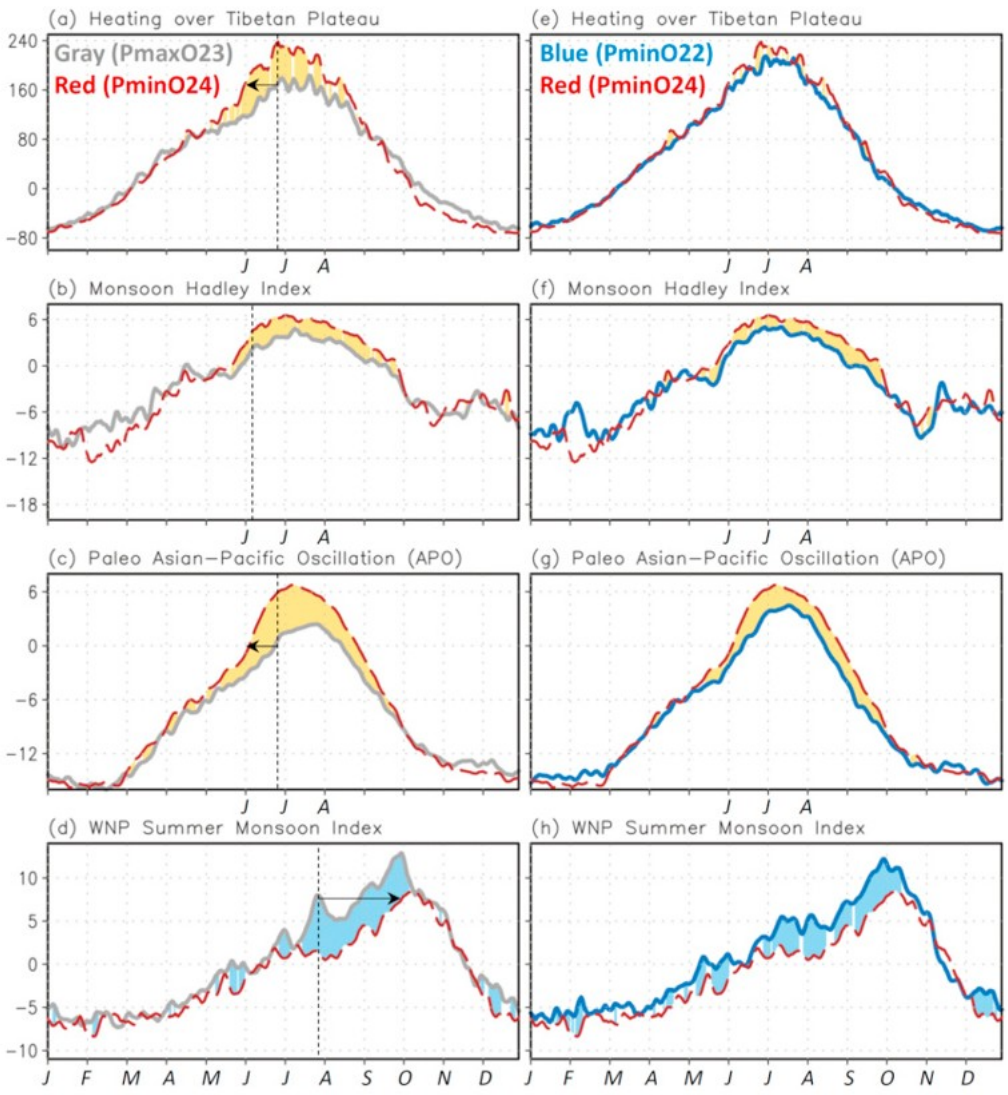

Fig. 2. Annual cycle of (a) the atmospheric column-integrated total heating (Wm^{-2}) over the Tibetan Plateau; (b) the monsoon Hadley index defined by the meridional wind shear ($m\ s^{-1}$) between 850 hPa and 200 hPa averaged over the region (70°E−110°E, 10°N–30°N); (c) the paleoclimate APO defined by the upper-tropospheric (500–200 hPa) temperature contrast (K) between regions (80°E−140°E, 35°N–55°N) and (150°E−150°W, 20°N–40°N); and (d) the WNP summer monsoon index defined by the difference in the 850-hPa westerlies ($m\ s^{-1}$) between regions (100°E−130°E, 5°N–15°N) and (110°E−140°E, 20°N–30°N). Solid gray (dashed red) lines denote the CAM/SOM PmaxO23 (PminO24) simulation, and shading denotes the PminO24 simulation minus the PmaxO23 simulation (yellow for a positive value in a–c and blue for a negative value in d, both with a confidence level of 90%). Same as (a–d) except with solid gray lines for the PminO22 simulation is shown in (e–h). (For interpretation of the references to color in this figure legend, the reader is referred to the Web version of this article.)

The combined effects of the WNP subtropical high and midlatitude westerly jet stream on the East Asian monsoon have been extensively investigated; for example, the intraseasonal Pacific–Japan (PJ) pattern (Kosaka and Nakamura, 2006; Nitta, 1987). The present-day Meiyu–Baiu season terminates in late July, coinciding with monsoon onset over the subtropical WNP (Suzuki and Hoskins, 2009; Wu et al., 2009a); the season is characterized by the deepening of the WNP monsoon trough and northward

shift of the WNP subtropical high. Recently, Wang et al. (2016) indicated that orbital-scale variations of the upper-tropospheric (500–200 hPa) temperature contrast between East Asia (80°E−140°E, 35°N–55°N) and the North Pacific region (150°E−150°W, 20°N–40°N) respond to precessional cycles; this contrast resembled the Asian–Pacific oscillation (APO) in today's interannual climate variability, and they defined an APO index to characterize it. As illustrated in Fig. 2c, the APO index is positive in late June in the control simulation, indicating an increase in zonally thermal contrast. This enhances the lower-tropospheric southerlies over East Asia, transporting moisture poleward and supporting the Meiyu–Baiu (refer to Fig. 4a and b). Influenced by early Holocene insolation, the APO index becomes positive approximately 1 month earlier, with a timing that matches the monsoon Hadley index and Tibetan Plateau heating in the PminO24 simulation. The enhanced lower-tropospheric southerly over East Asia, as a result of higher insolation and thermal contrast, corresponds to a stronger and westward-expanded WNP high (Wu et al., 2016a). Corresponding to the stronger WNP high, the WNP monsoon is absent in late July and August in PminO24 (Fig. 2d), as indicated by the monsoon trough index quantified according to the difference in the 850-hPa westerlies between regions (100°E−130°E, 5°N–15°N) and (110°E−140°E, 20°N–30°N) (Wang and Fan, 1999).

The aforementioned modeling results indicate that in boreal summer, the continental Asian monsoon intensifies whereas the maritime monsoon disappears because it is controlled by the early Holocene orbital setting. The land-sea heating contrast centered on the Tibetan Plateau intensifies and may consequently accelerate seasonal migration of the surrounding monsoons.

3.2. Migration of subtropical circulation and summer monsoons across Africa, Asia, and the WNP

This paper now focuses on the connection between the South Asian summer monsoon and the adjacent summer monsoons, particularly the causal relationship among the seasonal migrations of the monsoons. The early summer (May 15–June 15) and late summer (August) were selected to be investigated for specific details due to distinct characteristics of summer monsoon phases. Fig. 3, Fig. 4 present the precipitation and circulations in, respectively, the upper troposphere (velocity potentials) and lower troposphere (streamfunctions and streamlines). In the early summer, the center of the upper-tropospheric divergent circulation is over East and Southeast Asia and the Maritime Continent where heavy precipitation exists (Fig. 3a). Monsoon precipitation is maintained by the lower-tropospheric westerly and southwesterly flows over South Asia and East Asia, which are influenced by the competition of the South Asian monsoon low (negative streamfunction) and WNP subtropical high (positive streamfunction, Fig. 4a). Over Africa, an upper-tropospheric convergent circulation exists. The dipole in the velocity potential pattern is characteristic of broad-scale atmospheric circulation across Africa, South Asia, and the East Asia–WNP (Fig. 3a).

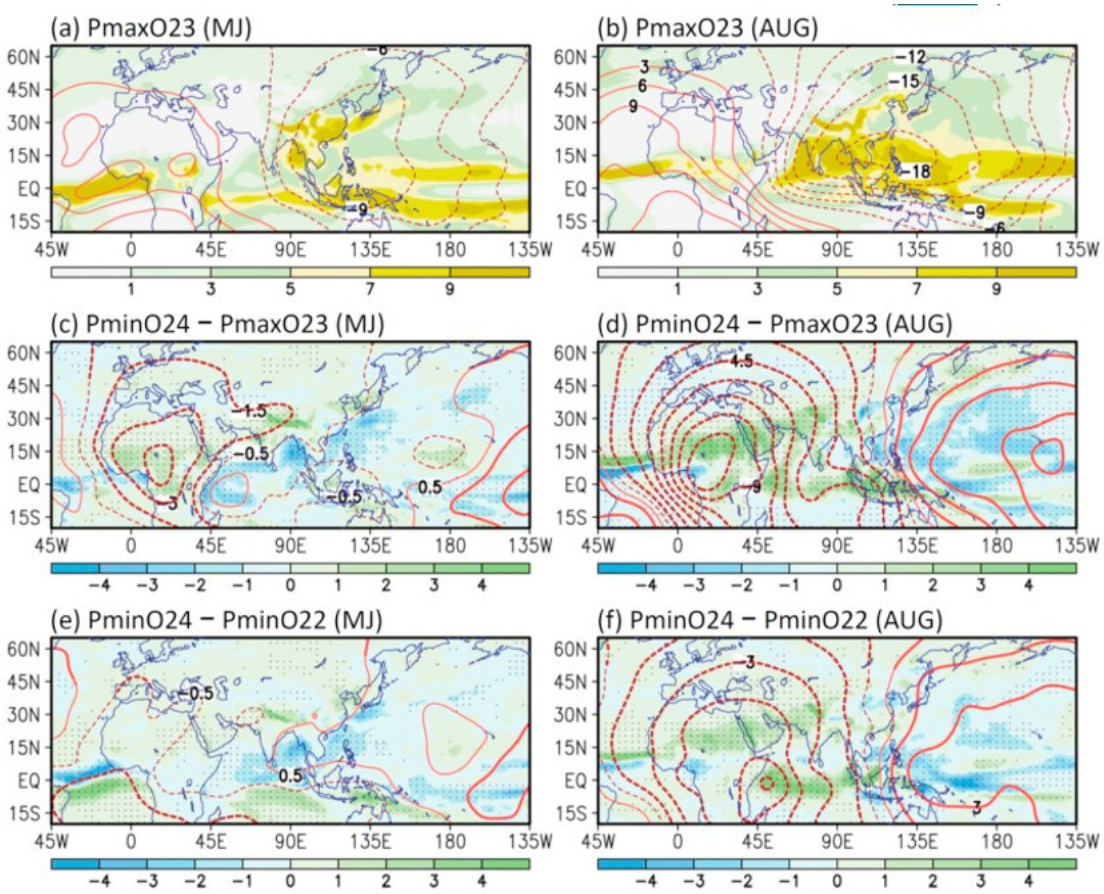

Fig. 3. Precipitation (shading, mm day^{-1}) and the 200-hPa velocity potential (contour lines, 10^6 m^2 s^{-1}) in the PmaxO23 simulation in (a) May 15–June 15 and (b) August. (c–d) Same as (a–b) but in PminO24 minus PmaxO23. Same as (a–b) but in PminO24 minus PminO22 is shown in (e–f). Thick contour lines and dots denote that the differences have a confidence level of 90%.

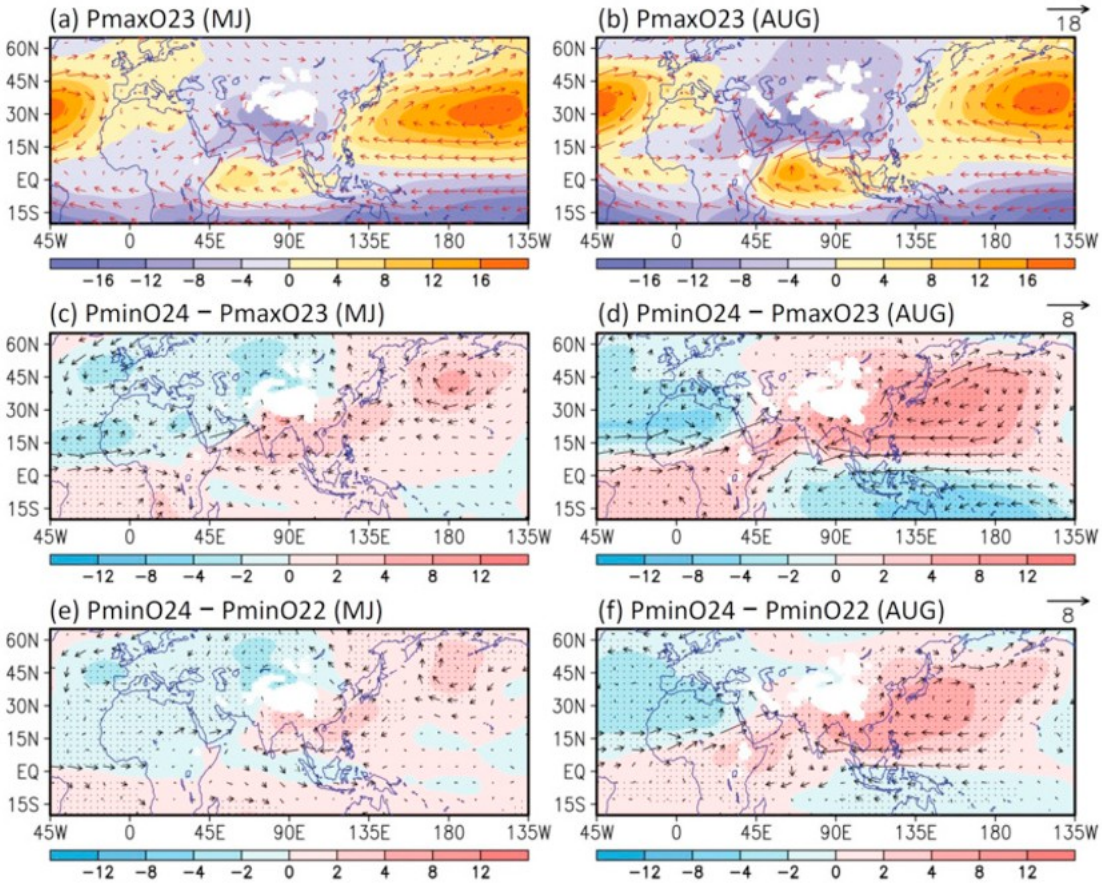

Fig. 4. Same as Fig. 3 except for the 850-hPa streamfunction (shading, $10^6\,m^2\,s^{-1}$) and winds (vectors, $m\,s^{-1}$).

In August, heavy precipitation occurs over the subtropical regions across West Africa, South Asia, and the subtropical WNP (Fig. 3b), and at locations further north than during the early summer. The East Asian precipitation penetrates further north to Korea and northeastern China. Now, the center region of the upper-tropospheric divergent circulation is located over India, the Bay of Bengal, the Indochina Peninsula, the South China Sea, and the subtropical WNP, characterizing another phase of the subtropical monsoon. In the lower troposphere, the monsoon low characterized by cyclonic circulation (negative streamfunction) expands zonally, marking the development of the monsoons in West Africa and the subtropical WNP (Fig. 4b).

In the early Holocene orbital forcing simulations (PminO24), early summer precipitation is increased over the African and Asian continents, whereas it is decreased over the northern Indian Ocean, Bay of Bengal, South China Sea, and WNP. The upper-tropospheric convergent circulation over Africa is weakened, with the largest decrease in velocity potentials occurring in Africa (Fig. 3c). Precipitation is shifted northwestward overall. The lower-tropospheric circulation difference between PminO24 and PmaxO23 (Fig. 4c) suggests that the anticyclonic circulation (with a positive streamfunction

anomaly) is attributable to the decrease in monsoon precipitation in the Bay of Bengal, South China Sea, and WNP. In contrast to the precipitation decrease slightly south of 20°N, the enhanced southerly flow may be responsible for the precipitation increase in the southern Tibetan Plateau–Himalayas and northern India. In West Africa, the lower-tropospheric cyclonic circulation (with a negative streamfunction anomaly) dynamically supports the increase in precipitation (Fig. 4c).

The orbitally driven monsoon changes are different in the early summer compared with late summer. In August, precipitation is greatly increased over the Asian and African continents, equatorial Indian Ocean, and Maritime Continent, whereas precipitation is decreased in the WNP. The precipitation changes relate to the reduced intensity of the upper-level dipole pattern in the velocity potential (Fig. 3d) and the westward expansion of the WNP high (Fig. 4d). Notably, the orbital response of tropical convection in August is opposite to that in early summer (compare Fig. 3c and d) and over the equatorial Indian Ocean versus the WNP in August (Fig. 3d). Potential mechanisms explaining this are discussed in later sections.

4. Relative influence of precession and obliquity during the early Holocene Asian summer monsoon

The differences between the PminO24 and PmaxO23 simulations include the combined effects of perihelion precession and high obliquity representing orbital differences between the early Holocene and present day. The PminO22 simulation was performed to determine the response to obliquity alone. Comparing Fig. 2e–h with Fig. 2a–d indicates that the effects of both obliquity and precession are considerable on the early Holocene Asian summer monsoon changes. Notably, as shown in Fig. 2e, a slight difference exists in the Tibetan Plateau heating responses to high versus low obliquity. It follows that precession has a primary impact on highland heating. As is shown later in this section, high obliquity can increase tropical heating; when obliquity-induced heating increases over the equatorial Indian Ocean, it competes with the precession-induced heating increase over the Tibetan Plateau and Maritime Continent.

In early summer, similar precipitation changes occur over the Asian summer monsoon region, induced either by only high obliquity or the combined orbital effect (perihelion precession and high obliquity). Over the northern Indian Ocean, Bay of Bengal, South China Sea, and WNP, high obliquity strongly reduces precipitation north of the equator in the early Holocene (compare Fig. 3c with Fig. 3e). With strong agreement in the monsoon precipitation changes (PminO24 vs. PmaxO23 or PminO22), an anomalously anticyclonic circulation exists in the lower troposphere over South and Southeast Asia (Fig. 4c–e). In the tropical region, the obliquity-induced precipitation change is increased south and decreased north of the equator (Fig. 3e); this differs from the changes caused by combined orbital effects. Fig. 5 further examines the corresponding changes in the

separate meridional circulations in the regions of 50°E−110°E and 110°E−140°E. Similar circulation responses occur over the monsoon region north of approximately 15°N between the two sets of orbital configurations (Fig. 5b vs. Fig. 5c; Fig. 5e vs. Fig. 5f). The upward motion strengthens at 25°N–30°N over land (50°E−110°E, Fig. 5b and c) and 30°N–40°N over the ocean (110°E−140°E, Fig. 5e and f), corresponding to the weakening of the midlatitude westerly jet stream (not shown). Differences over the tropics are considerable. When only the obliquity effect is included, the upward motion is greatly increased in the tropics south of the equator, whereas the upward motion is suppressed north of the equator (0–15°N). The subsidence anomaly may be simultaneously related to the sideway circulation anomaly (i.e., cyclonic in the north and anticyclonic in the south, Fig. 5c–f). Notably, only the subsidence anomaly exists between 15°S and 15°N when the precessional impact is included (Fig. 5b). Including the precessional impact enhances the convection over the Maritime Continent, as demonstrated by the increase in upward motion shown in Fig. 5e.

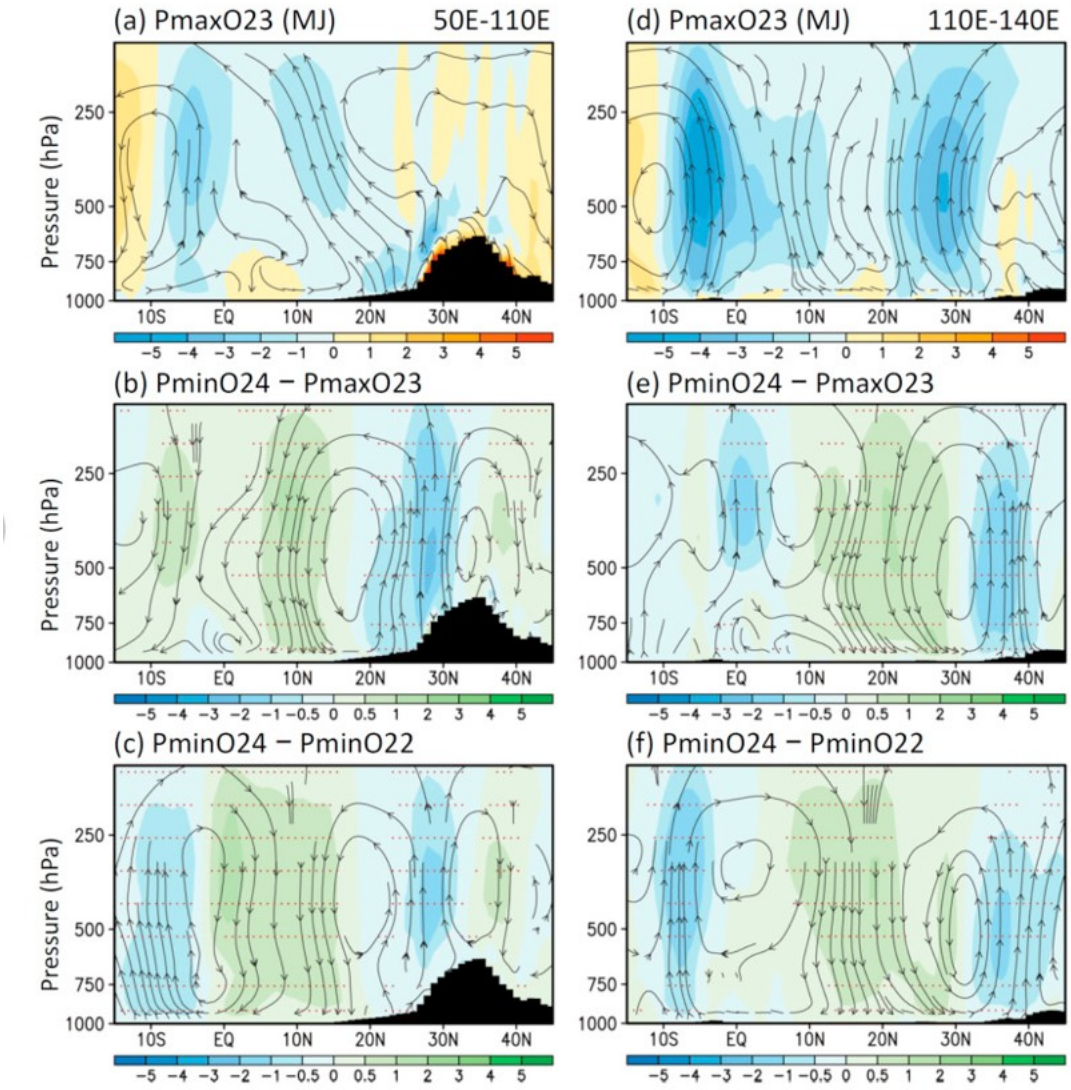

Fig. 5. Streamlines (the meridional component of divergent winds is used) and vertical velocity (colored, Pa min^{-1}) in (a) PmaxO23, (b) PminO24 minus PmaxO23, and (c) PminO24 minus PminO22 in the 50°E−110°E latitude–pressure plane from May 15 to June 15. Same as (a–c) except over 110°E−140°E is shown in (d–f). Black bars denote orography. Dots denote that the differences between vertical motions have a confidence level of 90%.

In August, a sizable candle-like heating over the Himalayas exists, as characterized by a strong upward motion (Fig. 6a), and is related to the strengthening of the lower-tropospheric monsoon flow (Fig. 4b). Across 50°E−110°E, the tropical precipitation and circulation responses to the two sets of orbital forcing conditions are similar in August (compare Fig. 3d with Fig. 3f; Fig. 6b with Fig. 6c), differing from those in early summer. High obliquity in August still substantially enhances the convective activity over the equatorial Indian Ocean (enhanced upward motion, Fig. 6a–c). In the 110°E−140°E section over the Maritime Continent, precession dominantly enhances convective activity; enhanced upward motion occurs only in the lower troposphere when forced only by high obliquity (compare Fig. 6e–f).

Regarding the effect of obliquity alone on tropical convection in the Indian Ocean–West Pacific, the zonally asymmetric response in August remains unclear (compare Fig. 6c–f).

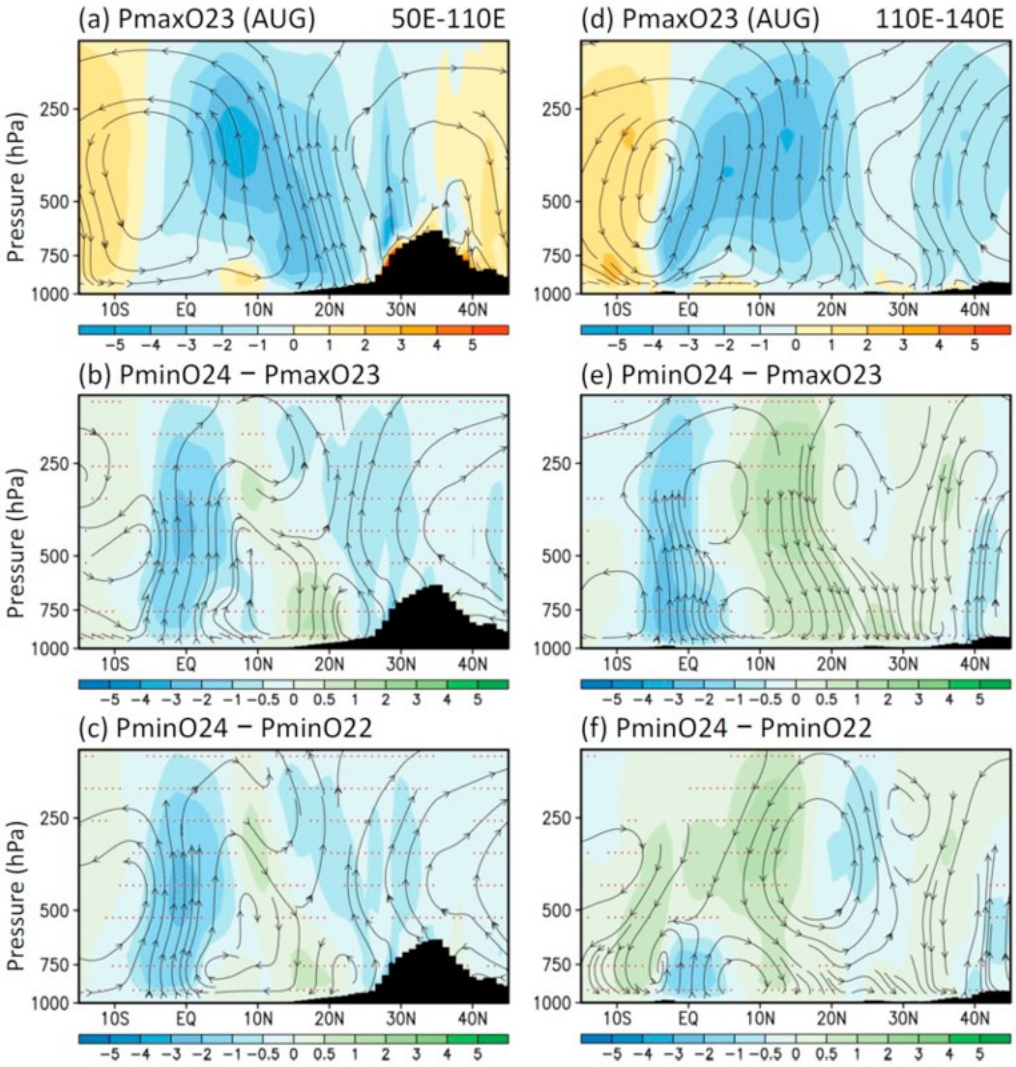

Fig. 6. Same as Fig. 5 but for in August.

4.1. Atmospheric heating changes in distinct monsoon regions

Fig. 7 illustrates the temporal evolution of the atmospheric (column-integrated) total heating and upper-tropospheric geopotential depth (200–500 hPa) in distinct monsoon regions (10°W–20°E, 50°E−110°E, 110°E−140°E). As shown in Fig. 7a–c, the PmaxO23 simulation captures the seasonality of contemporary monsoons with fidelity. Early summer Asian monsoon evolution and expanding subtropical circulation in August, both of which we focused on in this paper, are clearly identifiable. In West Africa, higher insolation causes earlier and further northward penetration of the summer monsoon (Fig. 7d). We discovered that higher obliquity substantially increases the geopotential depth in the upper troposphere of higher

latitudes, whereas only slight changes in the subtropical heating are induced (Fig. 7g). The modeling results suggest a precessional control of the African summer monsoon, which is consistent with the proxy data-based paradigm.

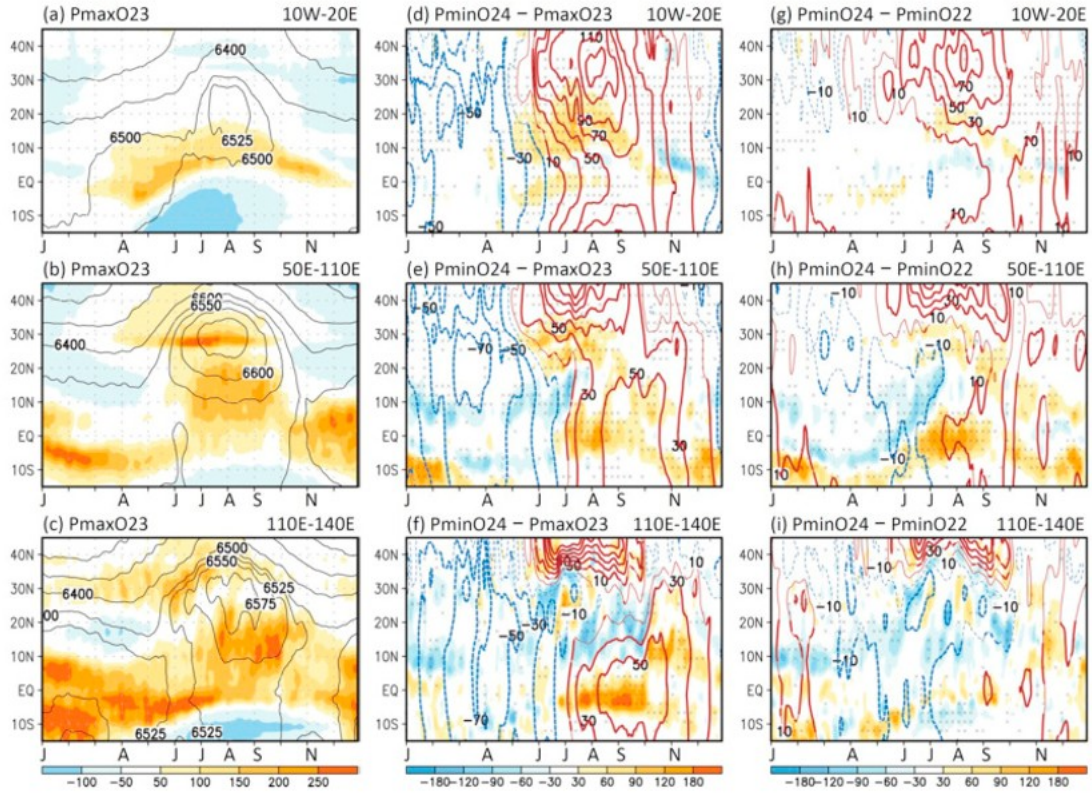

Fig. 7. Latitude–time cross sections of the atmospheric column-integrated total heating (colored, Wm^{-2}) and geopotential depth (gpm) between 500 hPa and 200 hPa of the PmaxO23 simulation at (a) 10°W–20°E, (b) 50°E−110°E, and (c) 110°E−140°E. Same as (a–c) except the results of PminO24 minus PmaxO23 are shown in (d–f) and PminO24 minus PminO22 are shown in (g–i).

Over South Asia and the Indian Ocean, higher insolation enhances the monsoonal heating over land (20°N–35°N) in late spring until summer and enhances the heating in the tropics in July–September. The increase in the upper-tropospheric geopotential depth is closely related to the heating increase (Fig. 7e), with distinct responses consistently displayed in the tropical regions relative to the monsoonal regions. The response to only obliquity forcing (Fig. 7h) further suggests the considerable impact of obliquity on tropical heating, whereas the associated heating changes are relatively small over 20°N–35°N. In the 50°E−110°E section, the perihelion precession appears to be primarily responsible for the increase in highland heating (including candle-like heating), whereas both perihelion precession and high obliquity enhance tropical condensational heating (refer to Fig. 3).

At 110°E−140°E, the combined orbital effects on heating and geopotential height are similar to those at 50°E−110°E, except for the candle-like heating (compare Fig. 7f with Fig. 7e). The increase in tropical heating in July–September is mostly attributable to the effect of perihelion precession over

the Maritime Continent rather than that of obliquity (compare Fig. 7f with Fig. 7i). In contrast to the combined orbital-induced increased heating over the Himalayas, Maritime Continent, and equatorial Indian Ocean, high obliquity alone appears to increase heating only over the equatorial Indian Ocean.

The following summary specifies the relative role of precession and obliquity in modulating the early Holocene Asian summer monsoon: (1) a combined effect of precession and obliquity enhances land-sea thermal contrast in East Asia; (2) precession dominates the enhancement of atmospheric heating over the Tibetan Plateau–Himalayas and Maritime Continent; and (3) obliquity considerably enhances the convection over the equatorial Indian Ocean. Furthermore, distinct orbital effects occur on the subseasonal timescale. In late spring and early summer, precession-induced heating increase over the Tibetan Plateau–Himalayas is most prominent. In July–August, precession greatly increases heating over the Tibetan Plateau–Himalayas, Maritime Continent, and equatorial Indian Ocean, whereas obliquity increases heating over the equatorial Indian Ocean.

5. Topographic modulation of the orbital-induced summer monsoon changes over and surrounding Asia

Large-scale topography, such as the Tibetan Plateau–Himalayas, has been considered a crucial element affecting the Asian monsoon (Kitoh, 2017; Molnar et al., 2010), with emphasis placed on both its mechanical and thermal contributions (Tada et al., 2016). On tectonic timescales, the Tibetan Plateau has been elevated and asynchronous responses of the East and South Asian summer monsoons have been noted (Tang et al., 2013). The Himalayas have a blocking effect on the summer monsoons in the surrounding region (Chen et al., 2014; Wu et al., 2018). Nevertheless, paleoclimate proxy records suggest that the summer monsoon might have penetrated further northward to Kunlun (northern Tibetan Plateau) during the Holocene (Ramisch et al., 2016). Topographic modulation of the orbital impact on regional to broad scale monsoon circulation has not yet been fully explored.

In the early Holocene, an increase in land-ocean thermal contrast caused by enhanced northern hemisphere summer insolation shifted the mean state of broad-scale monsoons to another phase. To further investigate the role of the Tibetan Plateau–Himalayas in modulating monsoonal response to orbital changes, simulations reducing the height of the region centered on the Plateau (45°E−125°E, 20°N–60°N) by 90% were performed. As previously described, we label these simulations as T0 experiments. We performed four simulations with orbital forcing matching the control, PmaxO23, PminO24, and PminO22. The T0 set of simulations provides insight into the blocking and thermal effects of high land on the monsoon and consequently any potential modulation in the associated orbital effects. We observed that with

a flat topography, monsoons are weaker and have a relatively slow seasonal evolution (PmaxO23_T0 compared with PmaxO23).

The T0 set of simulations also reveal that perihelion precession dramatically affects monsoon indices. With a low-altitude Tibetan Plateau, the monsoon indices under orbital forcing change in a similar manner as when the topography is unchanged (PmaxO23 vs. PminO24), although seasonal details of the monsoonal factors in PmaxO23_T0 are difficult to identify. For example, the Tibetan Plateau heating barely changes during summer and the APO becomes much weaker as its magnitude approaches 0 (not shown by figure). The effects of obliquity are also similar to those caused by the height-reduction of the Plateau (refer to Fig. 2e–h). Intriguingly, with a low-altitude Tibetan Plateau, obliquity has almost no impact on the early South Asian summer monsoon in June. The full-height Plateau intensifies the precessional strengthening of the South Asian summer monsoon (refer to Fig. 2f).

5.1. South Asian summer monsoon

Key features of the seasonal evolution of the South Asian summer monsoon circulation include strengthening of the lower-tropospheric southwesterly and southerly flow, buildup of the upper-tropospheric anticyclone, and development of a monsoon trough or low in the midtroposphere over the Bay of Bengal, south of the Himalayas, and over northern India. The mechanisms of monsoon evolution are closely related to the vertical coupling of these circulation components and are topographically dependent (Wu et al., 2014; Xie et al., 2006).

Renewed emphasis has recently been placed on the blocking effect of the Himalayas and the topographically induced condensational heating at the southern slope of the mountains, referred to as candle-like heating (Chen et al., 2014). Fig. 8 shows the meridional winds and vertical motion along 90°E. Associated with the arrival of the monsoonal southerly flow, a strong upward motion occurs over the southern Tibetan Plateau–Himalayas region. In the early summer, the southerly flow is located in the lower troposphere(e.g., speeds higher than $2\,m\,s^{-1}$ exist primarily at lower than 700 hPa, Fig. 8a). Higher insolation due to both precession and obliquity strengthens the southerly flow in front of the mountains and the upward motion (Fig. 8b). When influenced only by obliquity, the upward motion is slightly strengthened, with two separately increased southerly centers; near the surface and at approximately 600 hPa (Fig. 8c).
Anomalous subsidence occurs over the Tibetan Plateau when only under the control of obliquity.

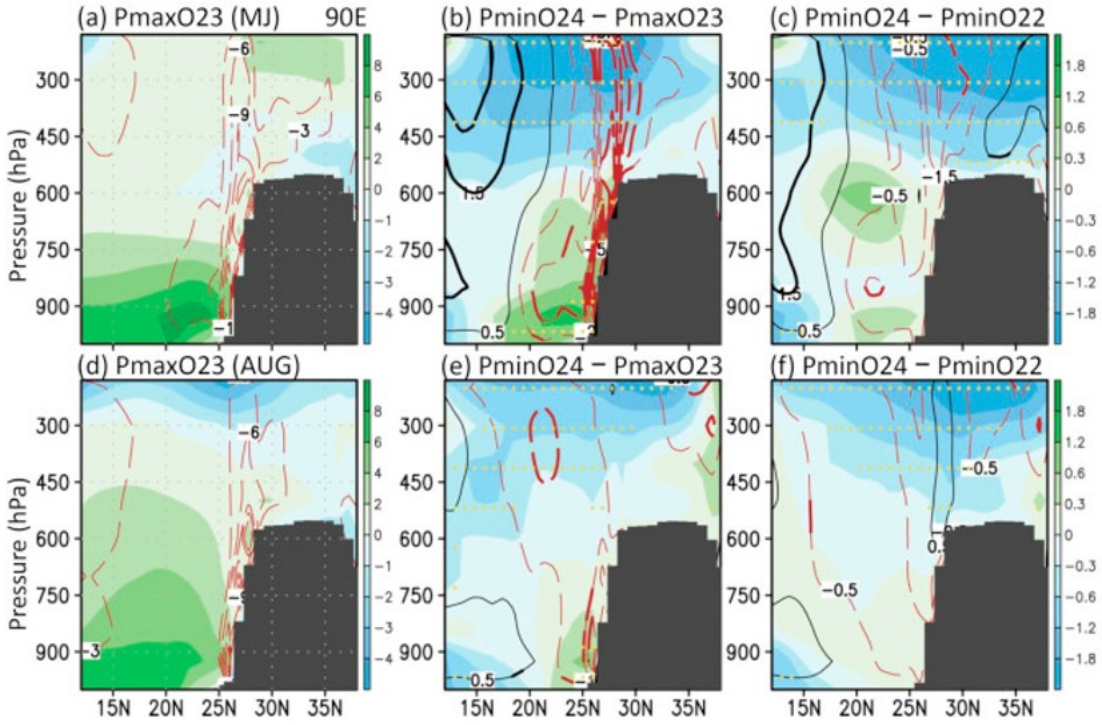

Fig. 8. Meridional wind speeds (shading, m s^{-1}) and vertical motion (contour lines, Pa min^{-1}) along 90°E: (a–c) May 15–June 15 of PmaxO23, PminO24 minus PmaxO23, and PminO24 minus PminO22, respectively; August of PmaxO23, PminO24 minus PmaxO23, and PminO24 minus PminO22 are shown in (d–f). Black bars denote topography, and positive contour lines indicating vertical motion are not displayed in (a) and (d). Thick contour lines and dots denote that the differences have a confidence level of 90%.

In August, the southerly flow deepens and can reach the 500 hPa level (e.g., speeds higher than 2 m s^{-1}, Fig. 8d). The precessional strengthening of the southerly and upward motion in front of the Himalayas remains apparent (Fig. 8e). Notably, anomalous subsidence exists over the Himalayas when only influenced by obliquity (Fig. 8f). Thus, precession is likely to be the primary modulator in the candle-like heating.

Fig. 9 further illustrates the latitude of the South Asian high center to facilitate examining the temporal evolution of the high. With a regular topography (Fig. 9a) and when influenced by early Holocene orbital forcing (PminO24), the upper-tropospheric high center penetrates further northward than it is presently positioned (over the Himalayas, PmaxO23). Thus, the blocking of the Himalayas, which has been considered a limiting factor in the meridional migration of the monsoon (Boos and Kuang, 2010; Wu et al., 2018), may not play a major role on the orbital timescale. High obliquity also shifts the center of the high. In the PminO22 simulation, the precessional forcing appears to be negated by low obliquity.

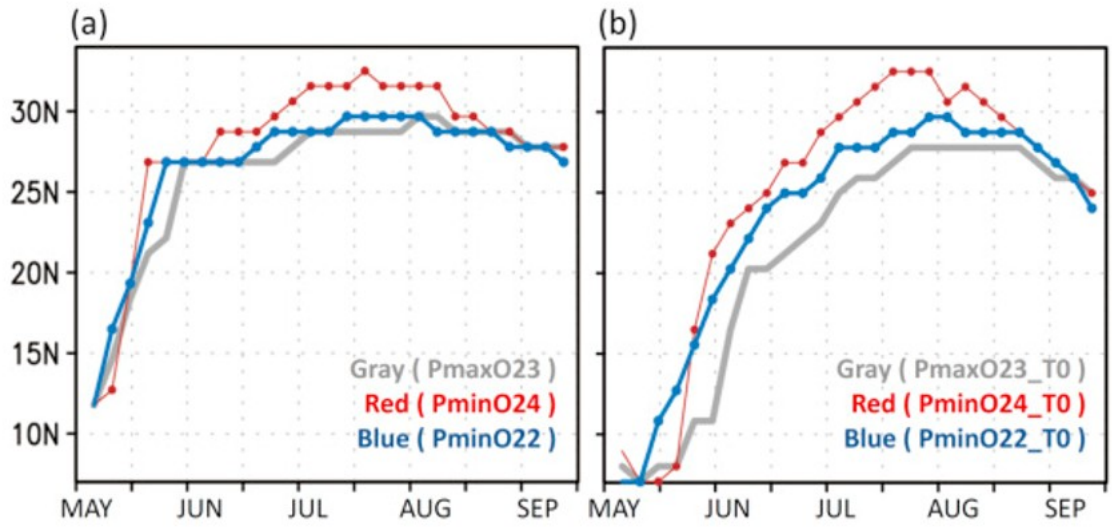

Fig. 9. Seasonal variation in the location of the South Asian high center at 200 hPa. Gray lines denote PmaxO23 and PmaxO23_T0 simulations; red lines with dots denote PminO24 and PminO24_T0 simulations; blue lines with dots denote PminO22 and PminO22_T0 simulations. The *x*-axis represents the period ranging from May to mid-September and an 11-day running mean has been applied. The interval between points is 5 days.

With low-altitude topography, the high center can still penetrate the region to the north of 25°N, although this occurs much later (Fig. 9b). Without the highland heating, precession still sizably shifts the upper-tropospheric high. Even with low obliquity, the effect of precessional forcing on shifting the high poleward is strong (PminO22_T0 vs. PmaxO23_T0, Fig. 9b), further suggesting that the existence of the Plateau intensifies the precessional impact. Furthermore, the high obliquity-induced poleward shifting of the high is considerable (PminO22_T0 vs. PminO24_T0, Fig. 9b).

5.2. Modulation of the large-scale circulation by the Plateau

Fig. 10 (to be compared with Fig. 4, Fig. 3) displays the circulation and precipitation features required for understanding topographic modulation in monsoon responses to orbital changes. We focus on August because the South Asian summer monsoon develops relatively slowly in the absence of the Plateau. For the present-day orbital condition (PmaxO23_T0), the lack of candle-like heating is expected; however, the precipitation in August is still considerable in southern Japan (Fig. 10a) and the WNP monsoon trough is insignificant (Fig. 10b). Regarding the combined effects of precession and obliquity, the Asian precipitation increases in the 20°N–45°N and 5°S–5°N sections, whereas it decreases in between them. This reduction in precipitation is prominent over the Arabian Sea, Bay of Bengal, South China Sea, and subtropical WNP (Fig. 10c), which differs from the response that occurs when the Plateau is included (Fig. 3d). The existence of the highlands appears to constrain the increase in precipitation in the subtropical region, partly by intensifying the candle-like heating. When only forced by obliquity, the competing effects on the tropical convection remain strong, as demonstrated by the enhanced heating over the equatorial Indian Ocean

(Fig. 10e) and Maritime Continent (Fig. 10c). Partly due to the weakened heating over land (i.e., absence of highland heating), the response of the WNP high to orbital changes is relatively weak (Fig. 10d–f). Thus, the existence of the Asian highlands may suppress the obliquity-induced Hadley circulation anomaly in South Asia–Indian Ocean (50°E−110°E).

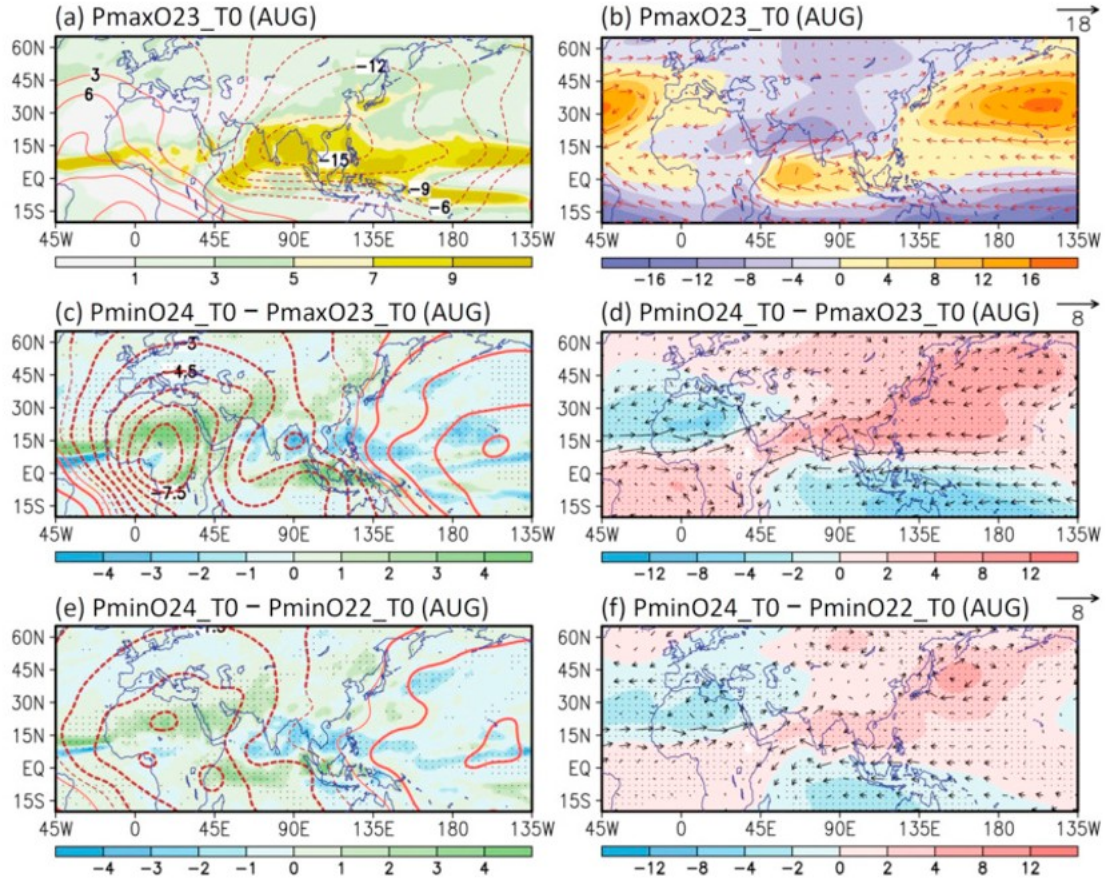

Fig. 10. Precipitation (shading, mm day^{-1}) and 200-hPa velocity potential (contour lines, 10^6 m^2 s^{-1}) in August: (a) PmaxO23_T0; (c) PminO24_T0 minus PmaxO23_T0; (e) PminO24_T0 minus PminO22_T0. Same as (a, c, e) except for the 850-hPa streamfunction (shading, 10^6 m^2 s^{-1}) and wind (vectors, m s^{-1}) are shown in (b, d, f). Thick contour lines and dots denote that the differences have a confidence level of 90%.

The anomalous Hadley circulation can be identified more clearly from the meridional circulation (Fig. 11, compared with Fig. 6). Without the highland heating, an anomalous ascending motion occurs in the 20°N–45°N and 5°S–5°N sections and a descending motion at 5°N–20°N in South Asia–Indian Ocean (50°E−110°E) (Fig. 11b and c), suggesting a strong Hadley-type circulation response. In today's climate, increased precipitation over the equatorial Indian Ocean in July and August is linked to the seasonal migration of African Sahel precipitation; the surrounding heating increase was demonstrated to weaken the South Asian monsoon (Wu et al., 2017a). Understanding the mechanisms that lead to the variability of the tropical convergence zone has been also considered a central problem in the study of the South Asian summer monsoon (Gadgil, 2003). We again suggest that

the existence of the Asian highlands may suppress the obliquity-induced Hadley circulation anomaly in South Asia–Indian Ocean.

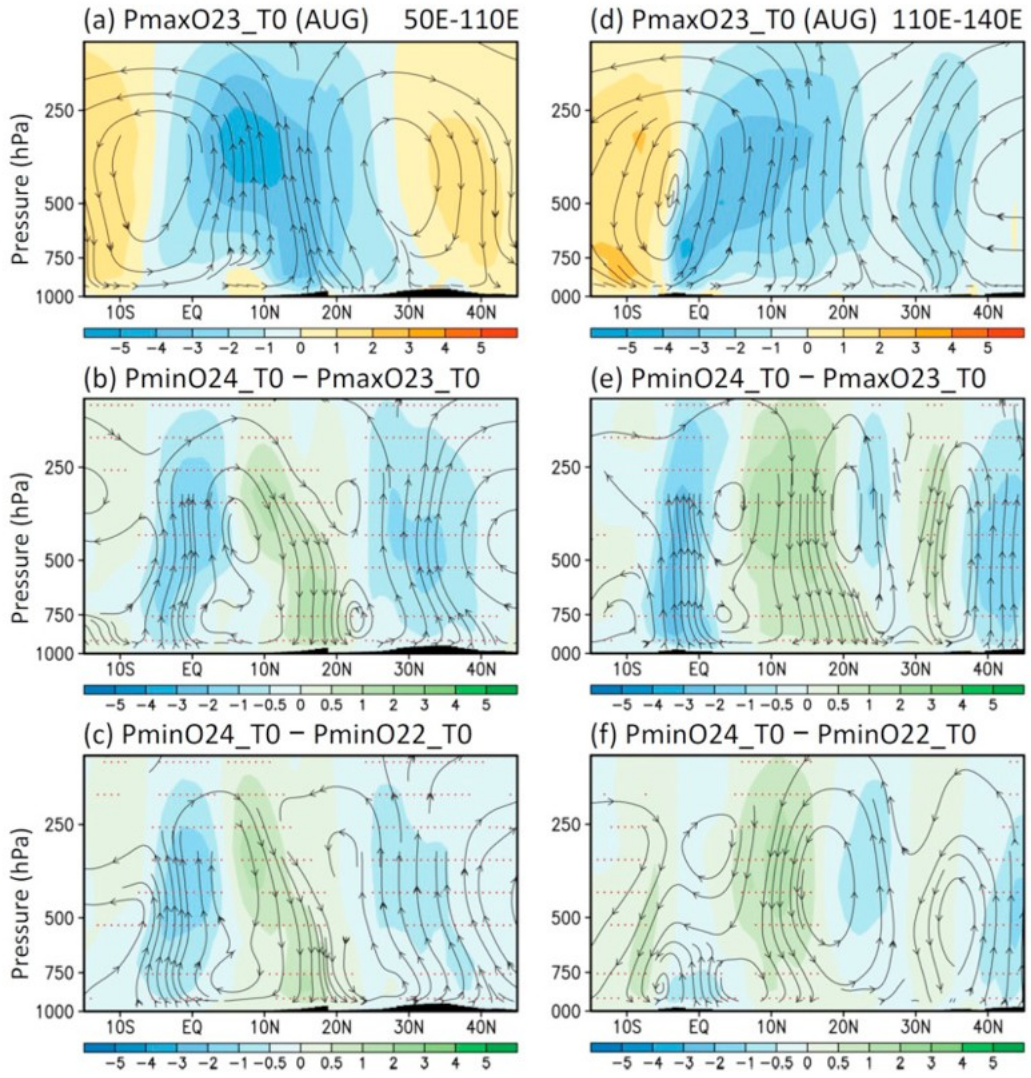

Fig. 11. Same as Fig. 6 except that the results of the T0 set of simulations are shown.

In contrast to the 50°E−110°E section, the circulation responses at 110°E−140°E with (Fig. 6e and f) and without (Fig. 11e and f) the full-height Plateau are similar. The precession-induced anomalous Hadley circulation may not be related to the existence of the highlands. Also, the atmospheric response over the Maritime Continent, which is the obliquity-forced convection change over the equatorial Indian Ocean, may have a remote influence through Walker-type circulation. Regarding the sea level rise during the Holocene (Griffiths et al., 2009; Siddall et al., 2003), any potential impact of Maritime Continent heating may have been underestimated because the sea level has been fixed at the present-day condition. However, even at a 100-km horizontal resolution, obtaining accurate convection and

precipitation simulations over the Maritime Continent remains challenging (Qian, 2008; Wu et al., 2017b).

6. Discussion and conclusions

6.1. Discussion

The equator-to-pole insolation gradient has been implicated in obliquity-scale precipitation changes in low latitudes, such as by forming a link to the strength of the African monsoon (Bosmans et al., 2015). Recent modeling results have further suggested similarities between obliquity- and global-warming-induced climate changes with regard also to the insolation gradient (Mantsis et al., 2014). However, determining the tropical origin of obliquity'scontrol remains a challenge. Although the results from idealized experiments have suggested the strong effects of obliquity in the tropical region, the proxy records have decisively indicated only a precessional signal (Cheng et al., 2012; Jin et al., 2014; Nagashima et al., 2013). In some cases, however, proxy records for the tropical Indian Ocean may follow the evolution of obliquity more clearly than that of precession (e.g., 90–75 and 45–30 ka BP). Regarding the orbital shaping of the monsoon seasonality, the modeling results of this study suggest that obliquity-induced changes in tropical convection can be crucial.

In addition, obliquity's impact was discovered to be constrained due to the existence of the Plateau. Our study provides insight into the topographic limit of obliquity forcing of monsoons. Orbital-scale monsoon changes driven by obliquity might be reasonably observed when the precession-induced inland and highland heating change is insignificant. Our finding aside, orbital control via the topographic effects on the monsoon are complex, and requires further study. In particular, a full oceanic feedback was lack of our simulations whether regarding the orbital or topographic effects.

Kutzbach et al. (2008) reported substantial phase lags of monsoon proxies to the changes of perihelion timing. For example, when perihelion has advanced to May, the land (ocean) temperature exhibits a lagged response to changes in orbital forcing in June (July). This lag response coincides with that of the seasonal insolation maxima. An important next step will be to explore the role of obliquity when the precessional change was small, e.g., to perform time-sliced simulations across 1 ka BP.

6.2. Conclusions

A series of climate simulations using the 1 × 1° CAM5 coupled with the SOM were performed to test the relative effects of a precession minimum and high obliquity in the early Holocene on the Asian summer monsoon. Under an early Holocene orbital condition, the Tibetan Plateau heating is increased and peaks approximately 1 month earlier (in late May instead of mid-to-late June); the continental Asian monsoon intensifies as a consequence. More broadly, the early summer precipitation is also increased over the African and Asian continents, whereas it is decreased over the northern Indian

Ocean, Bay of Bengal, South China Sea, and WNP. The overall northwestward shift of precipitation agrees with the paleoclimate proxy-based evidence.

In today's climate, heavy precipitation occurs in West Africa and in the subtropical WNP in July–August, during the late-summer phase of the subtropical monsoon. A large amount of convection also occurs over the equatorial Indian Ocean. Additionally, the upper-tropospheric anticyclonecentered on South Asia expands zonally. In contrast to the early summer monsoon phase being primarily controlled by inland and highland heating, late-summer monsoon phase is crucially affected by tropical and oceanic heating. The modeling results thus suggest differences in orbitally driven monsoon changes during the two distinct monsoon phases. Under early Holocene insolation, precipitation in August is greatly increased over the Asian and African continents, equatorial Indian Ocean, and Maritime Continent, whereas it is decreased in the WNP. In the late-summer monsoon phase, the orbitally driven changes in precipitation and upper-level divergent circulation show a considerable zonal contrast, separated by approximately 120°E.

The model-based diagnosis further suggests the relative effect of precession and obliquity during the early Holocene Asian summer monsoon and associated subseasonal dependence. Precession dominates atmospheric heating over the Tibetan Plateau–Himalayas and Maritime Continent (inland and highland origin), whereas obliquity mostly influences the heating over the equatorial Indian Ocean (tropical and oceanic origin). In early summer (Fig. 12a), the maximum precession and high obliquity are attributable to a northwestward shift and strengthening of the continental monsoon (Asia–Africa). However, distinct differences exist in the tropics. Precession enhances heating over the Maritime Continent and slightly reduces heating over the equatorial Indian Ocean; obliquity enhances the heating over the equatorial Indian Ocean, a competing effect to that of precession.

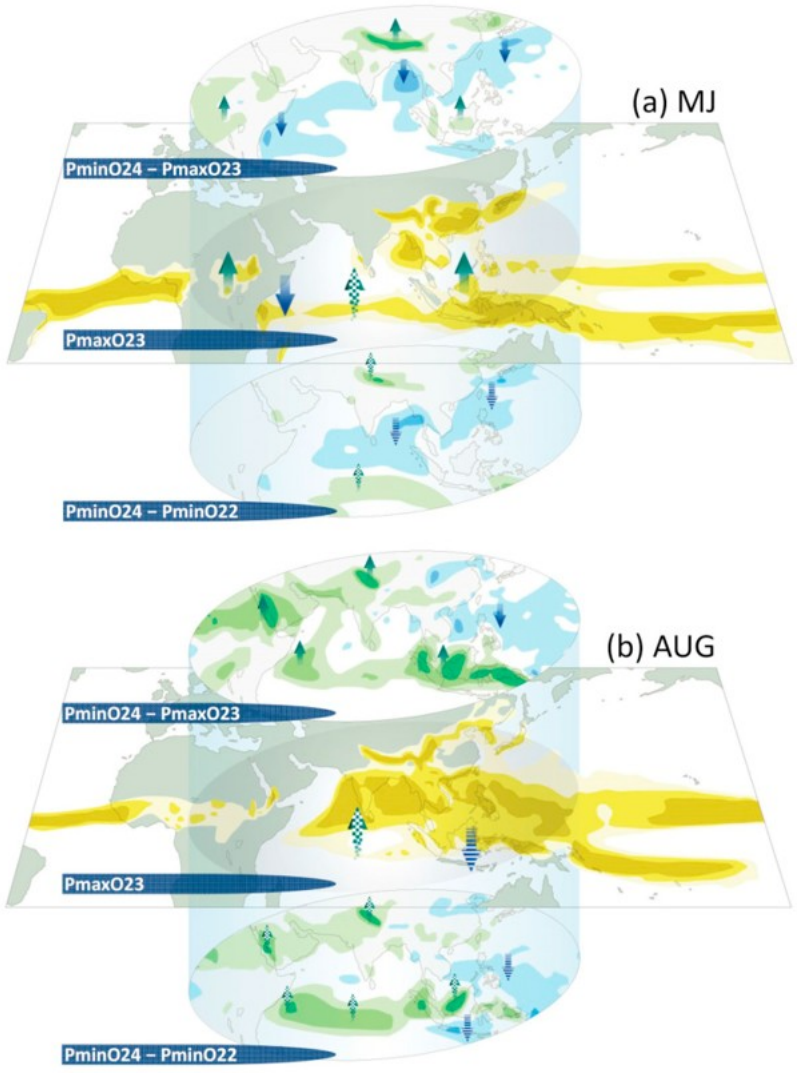

Fig. 12. Schematic of the relative effects of precession and obliquity (the shaded color refers to Fig. 3; arrows with full color denote PminO24 minus PmaxO23; arrows with grid points or lines denote PminO24 minus PminO22); only different responses between PminO24 minus PmaxO23 and PminO24 minus PminO22 are marked in PmaxO23 (middle panels). In the early summer (a), the minimum precession and high obliquity are attributable to the northwestward shift and strengthening of the continental monsoon in Asia–Africa. In the tropics, precession enhances heating primarily over the Maritime Continent, whereas obliquity enhances heating mostly over the equatorial Indian Ocean, suggesting a competing role. By August (b), the Asian monsoon has shifted southeastward. Obliquity critically enhances the peak value of precipitation and convection in the equatorial Indian Ocean. A competing effect of precession and obliquity exists for reducing zonal heating contrast in the tropics.

The overall Asian monsoon shifts southeastward in August (compare middle panels in Fig. 12a–b). Precession and obliquity still play contracting roles in driving orbital-scale monsoon changes (Fig. 12b). The present-day effects of obliquity in the tropics include the peak value of atmospheric heating in the tropical Indian Ocean. Regarding the heating changes over the tropical Indian Ocean and Maritime Continent, obliquity may reduce the zonal

heating difference. The individual effect of precession and obliquity may thus be modulated.

Potential topographic modulation of the orbitally-driven monsoon changes was investigated through simulations changing the orbital parameters as before, but using model topography that removed the highland regioncentered on the Plateau. The results suggest that the existence of the Plateau intensifies the precessional impact, with precession forcing shifting the upper-tropospheric South Asian anticyclone northwards for example. By contrast, with increased obliquity the meridional circulation is suppressed over the South Asia–Indian Ocean. Without a Tibetan Plateau and the consequent sizable reduction in the highland heating in the South Asia–Indian Ocean (50°E−110°E) sector, higher obliquity drives stronger ascending motion over the equatorial region (5°S–5°N) and stronger descending motion over the northern tropics/subtropics (5°N–20°N), thus suppressing the subtropical monsoon (Fig. 10e). By contrast, only zonal asymmetric precipitation change occurs in response to obliquity when the topography is present (Fig. 3f).

Acknowledgments

This work was supported by the Consortium for Climate Change Study (CCliCS) and CMIP6 Taiwan under the auspices of the Ministry of Science and Technology, Taiwan, under grants MOST 106–2111–M–001–004–, 106–2111–M–001–005–, and 106–2611–M–001–001–. JCHC was funded by National Science Foundation grant AGS–1405479. We are grateful to the National Center for Atmospheric Research for making the CESM model accessible to the community; and the National Center for High-Performance Computing (NCHC) for supercomputer resources. Thanks also go to Ms. Hai-Wei Lin for preparing the schematic diagram in Fig. 12.

References

An, 2000

Z.S. An**The history and variability of the East Asian paleomonsoon climate**

Quat. Sci. Rev., 19 (2000), pp. 171-187

An et al., 2015

Z.S. An, G.X. Wu, J.P. Li, Y.B. Sun, Y.M. Liu, W.J. Zhou, Y.J. Cai, A.M. Duan, L.Li, J.Y. Mao, H. Cheng, Z.G. Shi, L.C. Tan, H. Yan, H. Ao, H. Chang, J. Feng**Global monsoon dynamics and climate change**

Annu. Rev. Earth Planet Sci., 43 (43) (2015), pp. 29-77

Anderson and Prell, 1993

D.M. Anderson, W.L. Prell**A 300 Kyr record of upwelling off Oman during the late quaternary - evidence of the asian southwest monsoon**

Paleoceanography, 8 (1993), pp. 193-208

Battisti et al., 2014

D.S. Battisti, Q.H. Ding, G.H. Roe**Coherent pan-Asian climatic and isotopic response to orbital forcing of tropical insolation**

J. Geophys. Res. Atmos., 119 (2014), pp. 11997-12020

Boos and Kuang, 2010

W.R. Boos, Z. Kuang**Dominant control of the South Asian monsoon by orographic insulation versus plateau heating**

Nature, 463 (2010), pp. 218-222

Bosmans et al., 2015

J.H.C. Bosmans, F.J. Hilgen, E. Tuenter, L.J. Lourens**Obliquity forcing of low-latitude climate**

Clim. Past, 11 (2015), pp. 1335-1346

Braconnot and Marti, 2003

P. Braconnot, O. Marti**Impact of precession on monsoon characteristics from coupled ocean atmosphere experiments: changes in Indian monsoon and Indian ocean climatology**

Mar. Geol., 201 (2003), pp. 23-34

Braconnot et al., 2008

P. Braconnot, C. Marzin, L. Gregoire, E. Mosquet, O. Marti**Monsoon response to changes in Earth's orbital parameters: comparisons between simulations of the Eemian and of the Holocene**

Clim. Past, 4 (2008), pp. 281-294

Cai et al., 2017

Y.J. Cai, J.C.H. Chiang, S.F.M. Breitenbach, L.C. Tan, H. Cheng, R.L.Edwards, Z. S. An**Holocene moisture changes in western China, Central Asia, inferred from stalagmites**

Quat. Sci. Rev., 158 (2017), pp. 15-28

Caley et al., 2011

T. Caley, B. Malaize, M. Revel, E. Ducassou, K. Wainer, M. Ibrahim, D.Shoeaib, S. Migeon, V. Marieu**Orbital timing of the Indian, East Asian and African boreal monsoons and the concept of a 'global monsoon'**

Quat. Sci. Rev., 30 (2011), pp. 3705-3715

Caley et al., 2014

T. Caley, D.M. Roche, H. Renssen**Orbital Asian summer monsoon dynamics revealed using an isotope- enabled global climate model**

Nat. Commun., 5 (2014), p. 5371

Carolin et al., 2016

S.A. Carolin, K.M. Cobb, J. Lynch-Stieglitz, J.W. Moerman, J.W. Partin, S.Lejau, J. Malang, B. Clark, A.A. Tuen, J.F. Adkins**Northern Borneo stalagmite records reveal West Pacific hydroclimate across MIS 5 and 6**

Earth Planet Sci. Lett., 439 (2016), pp. 182-193

Chen et al., 2014

G.S. Chen, Z. Liu, J.E. Kutzbach**Reexamining the barrier effect of the Tibetan Plateau on the South Asian summer monsoon**

Clim. Past, 10 (2014), pp. 1269-1275

Cheng et al., 2012

H. Cheng, A. Sinha, X.F. Wang, F.W. Cruz, R.L. Edwards**The global paleomonsoon as seen through speleothem records from Asia and the Americas**

Clim. Dynam., 39 (2012), pp. 1045-1062

Chiang et al., 2015

J.C.H. Chiang, I.Y. Fung, C.H. Wu, Y.H. Cai, J.P. Edman, Y.W. Liu, J.A.Day, T. Bh attacharya, Y. Mondal, C.A. Labrousse**Role of seasonal transitions and westerly jets in East Asian paleoclimate**

Quat. Sci. Rev., 108 (2015), pp. 111-129

Choudhury and Krishnan, 2011

A.D. Choudhury, R. Krishnan**Dynamical response of the south asian monsoon trough to latent heating from stratiform and convective precipitation**

J. Atmos. Sci., 68 (2011), pp. 1347-1363

Dallmeyer et al., 2010

A. Dallmeyer, M. Claussen, J. Otto**Contribution of oceanic and vegetation feedbacks to Holocene climate change in monsoonal Asia**

Clim. Past, 6 (2010), pp. 195-218

Dallmeyer et al., 2013

A. Dallmeyer, M. Claussen, Y. Wang, U. Herzschuh**Spatial variability of Holocene changes in the annual precipitation pattern: a model-data synthesis for the Asian monsoon region**

Clim. Dynam., 40 (2013), pp. 2919-2936

Danabasoglu and Gent, 2009

G. Danabasoglu, P.R. Gent**Equilibrium climate sensitivity: is it accurate to use a slab ocean model?**

J. Clim., 22 (2009), pp. 2494-2499

Dayem et al., 2010

K.E. Dayem, P. Molnar, D.S. Battisti, G.H. Roe**Lessons learned from oxygen isotopes in modern precipitation applied to interpretation of speleothem records of paleoclimate from eastern Asia**

Earth Planet Sci. Lett., 295 (2010), pp. 219-230

Duan and Wu, 2005

A.M. Duan, G.X. Wu**Role of the Tibetan Plateau thermal forcing in the summer climate patterns over subtropical Asia**

Clim. Dynam., 24 (2005), pp. 793-807

Fleitmann et al., 2007

D. Fleitmann, S.J. Burns, A. Mangini, M. Mudelsee, J. Kramers, I. Villa, U. Neff, A.A. Al-Subbary, A. Buettner, D. Hippler, A. Matter**Holocene ITCZ and Indian monsoon dynamics recorded in stalagmites from Oman and Yemen (Socotra)**

Quat. Sci. Rev., 26 (2007), pp. 170-188

Gadgil, 2003

S. Gadgil**The Indian monsoon and its variability**

Annu. Rev. Earth Planet Sci., 31 (2003), pp. 429-467

Gibbons et al., 2014

F.T. Gibbons, D.W. Oppo, M. Mohtadi, Y. Rosenthal, J. Cheng, Z. Liu, B.K. Linsley**Deglacial δ18O and hydrologic variability in the tropical Pacific and indian oceans**

Earth Planet Sci. Lett., 387 (2014), pp. 240-251

Goswami et al., 1999

B.N. Goswami, V. Krishnamurthy, H. Annamalai**A broad-scale circulation index for the interannual variability of the Indian summer monsoon**

Q. J. R. Meteorol. Soc., 125 (1999), pp. 611-633

Griffiths et al., 2009

M.L. Griffiths, R.N. Drysdale, M.K. Gagan, J.X. Zhao, L.K. Ayliffe, J.C.Hellstrom, W.S. Hantoro, S. Frisia, Y.X. Feng, I. Cartwright, E.S. Pierre, M.J. Fischer, B.W. Suwargadi**Increasing Australian-Indonesian monsoon rainfall linked to early Holocene sea-level rise**

Nat. Geosci., 2 (2009), pp. 636-639

Hsu and Liu, 2003

H.H. Hsu, X. Liu**Relationship between the Tibetan plateau heating and east Asian summer monsoon rainfall**

Geophys. Res. Lett., 30 (2003)

Jin et al., 2014

L. Jin, B. Schneider, W. Park, M. Latif, V. Khon, X. Zhang**The spatial–temporal patterns of Asian summer monsoon precipitation in response to Holocene insolation change: a model-data synthesis**

Quat. Sci. Rev., 85 (2014), pp. 47-62

Jung et al., 2009

S.J.A. Jung, D. Kroon, G. Ganssen, F. Peeters, R. Ganeshram**Enhanced Arabian Sea intermediate water flow during glacial North Atlantic cold phases**

Earth Planet Sci. Lett., 280 (2009), pp. 220-228

Kathayat et al., 2016

G. Kathayat, H. Cheng, A. Sinha, C. Spotl, R.L. Edwards, H. Zhang, X.Li, L. Yi, Y. Ning, Y. Cai, W.L. Lui, S.F. Breitenbach**Indian monsoon variability on millennial-orbital timescales**

Sci. Rep., 6 (2016), p. 24374

Kitoh, 2002

A. Kitoh**Effects of large-scale mountains on surface climate - a coupled ocean-atmosphere general circulation model study**

J. Meteorol. Soc. Jpn., 80 (2002), pp. 1165-1181

Kitoh, 2017

A. Kitoh**The asian monsoon and its future change in climate models: a review**

J. Meteorol. Soc. Jpn., 95 (2017), pp. 7-33

Kosaka and Nakamura, 2006

Y. Kosaka, H. Nakamura**Structure and dynamics of the summertime Pacific–Japan teleconnection pattern**

Q. J. R. Meteorol. Soc., 132 (2006), pp. 2009-2030

Kutzbach et al., 2008

J.E. Kutzbach, X. Liu, Z. Liu, G. Chen**Simulation of the evolutionary response of global summer monsoons to orbital forcing over the past 280,000 years**

Clim. Dynam., 30 (2008), pp. 567-579

Lee and Poulsen, 2009

S.Y. Lee, C.J. Poulsen**Obliquity and precessional forcing of continental snow fall and melt: implications for orbital forcing of Pleistocene ice ages**

Quat. Sci. Rev., 28 (2009), pp. 2663-2674

Liu et al., 2003

X.D. Liu, J.E. Kutzbach, Z.Y. Liu, Z.S. An, L. Li**The Tibetan Plateau as amplifier of orbital-scale variability of the East Asian monsoon**

Geophys. Res. Lett., 30 (2003)

Liu et al., 2015

Y. Liu, L. Lo, Z. Shi, K.Y. Wei, C.J. Chou, Y.C. Chen, C.K. Chuang, C.C. Wu, H.S. Mii, Z. Peng, H. Amakawa, G.S. Burr, S.Y. Lee, K.L. DeLong, H. Elderfield, C.C. Shen**Obliquity pacing of the western Pacific intertropical convergence zone over the past 282,000 years**

Nat. Commun., 6 (2015), p. 10018

Liu et al., 2004

Z. Liu, S.P. Harrison, J. Kutzbach, B. Otto-Bliesner**Global monsoons in the mid-Holocene and oceanic feedback**

Clim. Dynam., 22 (2004), pp. 157-182

Mantsis et al., 2014

D.F. Mantsis, B.R. Lintner, A.J. Broccoli, M.P. Erb, A.C. Clement, H.S.Park**The response of large-scale circulation to obliquity-induced changes in meridional heating gradients**

J. Clim., 27 (2014), pp. 5504-5516

Merlis et al., 2013

T.M. Merlis, T. Schneider, S. Bordoni, I. Eisenman**The tropical precipitation response to orbital precession**

J. Clim., 26 (2013), pp. 2010-2021

Mohtadi et al., 2010

M. Mohtadi, A. Luckge, S. Steinke, J. Groeneveld, D. Hebbeln, N.Westphal**Lat e Pleistocene surface and thermocline conditions of the eastern tropical Indian Ocean**

Quat. Sci. Rev., 29 (2010), pp. 887-896

Mohtadi et al., 2016

M. Mohtadi, M. Prange, S. Steinke**Palaeoclimatic insights into forcing and response of monsoon rainfall**

Nature, 533 (2016), pp. 191-199

Molnar et al., 2010

P. Molnar, W.R. Boos, D.S. Battisti**Orographic controls on climate and paleoclimate of Asia: thermal and mechanical roles for the Tibetan plateau**

Annu. Rev. Earth Planet Sci., 38 (2010), pp. 77-102

Nagashima et al., 2013

K. Nagashima, R. Tada, S. Toyoda**Westerly jet-East Asian summer monsoon connection during the Holocene**

G-cubed, 14 (2013), pp. 5041-5053

Nitta, 1987

T. Nitta**Convective activities in the tropical western Pacific and their impact on the northern-hemisphere summer circulation**

J. Meteorol. Soc. Jpn., 65 (1987), pp. 373-390

Qian, 2008

J.H. Qian**Why precipitation is mostly concentrated over islands in the Maritime Continent**

J. Atmos. Sci., 65 (2008), pp. 1428-1441

Rachmayani et al., 2015

R. Rachmayani, M. Prange, M. Schulz**North African vegetation–precipitation feedback in early and mid-Holocene climate simulations with CCSM3-DGVM**

Clim. Past, 11 (2015), pp. 175-185

Rachmayani et al., 2016

R. Rachmayani, M. Prange, M. Schulz**Intra-interglacial climate variability: model simulations of Marine Isotope Stages 1, 5, 11, 13, and 15**

Clim. Past, 12 (2016), pp. 677-695

Ramisch et al., 2016

A. Ramisch, G. Lockot, T. Haberzettl, K. Hartmann, G. Kuhn, F.Lehmkuhl, S. S chimpf, P. Schulte, G. Stauch, R. Wang, B. Wunnemann, D. Yan, Y.Zhang, B. Diekmann**A persistent northern boundary of indian summer monsoon precipitation over central Asia during the Holocene**

Sci. Rep., 6 (2016), p. 25791

Rodwell and Hoskins, 1996

M.J. Rodwell, B.J. Hoskins**Monsoons and the dynamics of deserts**

Q. J. R. Meteorol. Soc., 122 (1996), pp. 1385-1404

Rodwell and Hoskins, 2001

M.J. Rodwell, B.J. Hoskins**Subtropical anticyclones and summer monsoons**

J. Clim., 14 (2001), pp. 3192-3211

Saraswat et al., 2013

R. Saraswat, D.W. Lea, R. Nigam, A. Mackensen, D.K. Naik**Deglaciation in the tropical Indian Ocean driven by interplay between the regional monsoon and global teleconnections**

Earth Planet Sci. Lett., 375 (2013), pp. 166-175

Saraswat et al., 2005

R. Saraswat, R. Nigam, S. Weldeab, A. Mackensen, P.D. Naidu**A first look at past sea surface temperatures in the equatorial Indian Ocean from Mg/Ca in foraminifera**

Geophys. Res. Lett., 32 (2005)

Shi et al., 2012

Z. Shi, X. Liu, X. Cheng**Anti-phased response of northern and southern East Asian summer precipitation to ENSO modulation of orbital forcing**

Quat. Sci. Rev., 40 (2012), pp. 30-38

Shi et al., 2011

Z.G. Shi, X.D. Liu, Y.B. Sun, Z.S. An, Z. Liu, J. Kutzbach**Distinct responses of East Asian summer and winter monsoons to astronomical forcing**

Clim. Past, 7 (2011), pp. 1363-1370

Siddall et al., 2003

M. Siddall, E.J. Rohling, A. Almogi-Labin, C. Hemleben, D. Meischner, I.Schmel zer, D.A. Smeed**Sea-level fluctuations during the last glacial cycle**

Nature, 423 (2003), pp. 853-858

Stott et al., 2002

L. Stott, C. Poulsen, S. Lund, R. Thunell**Super ENSO and global climate oscillations at millennial time scales**

Science, 297 (2002), p. 222

Suzuki and Hoskins, 2009

S. Suzuki, B. Hoskins**The large-scale circulation change at the end of the Baiu season in Japan as seen in ERA40 data**

J. Meteorol. Soc. Jpn., 87 (2009), pp. 83-99

Tada et al., 2016

R. Tada, H.B. Zheng, P.D. Clift**Evolution and variability of the Asian monsoon and its potential linkage with uplift of the Himalaya and Tibetan Plateau**

prog. earth. plannet. sci, 3 (2016), pp. 1-26

Tang et al., 2013

H. Tang, A. Micheels, J.T. Eronen, B. Ahrens, M. Fortelius**Asynchronous responses of East Asian and Indian summer monsoons to mountain uplift shown by regional climate modelling experiments**

Clim. Dynam., 40 (2013), pp. 1531-1549

Tuenter et al., 2003

E. Tuenter, S.L. Weber, F.J. Hilgen, L.J. Lourens**The response of the African summer monsoon to remote and local forcing due to precession and obliquity**

Global Planet. Change, 36 (2003), pp. 219-235

Vertenstein et al., 2010

M.T.C. Vertenstein, A. Middleton, D. Feddema, C. Fischer**CESM1.0.3 User's Guide**

(2010)

available at:

http://www.cesm.ucar.edu/

Wang and Fan, 1999

B. Wang, Z. Fan**Choice of south Asian summer monsoon indices**

Bull. Am. Meteorol. Soc., 80 (1999), pp. 629-638

Wang et al., 2016

Y. Wang, Z. Jian, P. Zhao, D. Xiao, J. Chen**Relative roles of land- and ocean-atmosphere interactions in Asian-Pacific thermal contrast variability at the precessional band**

Sci. Rep., 6 (2016), p. 28349

Wu et al., 2018

C.-H. Wu, M.-D. Chou, Y.-H. Fong**Impact of the Himalayas on the meiyu–Baiu migration**

Clim. Dynam., 50 (2018), pp. 1307-1319

Wu and Hsu, 2016

C.-H. Wu, H.-H. Hsu**Role of the Indochina Peninsula narrow mountains in modulating the east Asian–Western North Pacific summer monsoon**

J. Clim., 29 (2016), pp. 4445-4459

Wu et al., 2017a

C.-H. Wu, S.Y.S. Wang, H.-H. Hsu**Large-scale control of the Arabian Sea monsoon inversion in August**

Clim. Dynam. (2017), 10.1007/s00382-017-4029-7

(in press)

Wu et al., 2016a

C.H. Wu, J.C.H. Chiang, H.H. Hsu, S.Y. Lee**Orbital control of the western North Pacific summer monsoon**

Clim. Dynam., 46 (2016), pp. 897-911

Wu et al., 2017b

C.H. Wu, N. Freychet, C.A. Chen, H.H. Hsu**East Asian presummer precipitation in the CMIP5 at high versus low horizontal resolution**

Int. J. Climatol., 37 (2017), pp. 4158-4170

Wu et al., 2014

C.H. Wu, H.H. Hsu, M.D. Chou**Effect of the Arakan mountains in the northwestern Indochina Peninsula on the late may asian monsoon transition**

J. Geophys. Res. Atmos., 119 (2014), pp. 10769-10779

Wu et al., 2009a

C.H. Wu, W.S. Kau, M.D. Chou**Summer monsoon onset in the subtropical western North Pacific**

Geophys. Res. Lett., 36 (2009)

Wu et al., 2016b

C.H. Wu, S.Y. Lee, J.C.H. Chiang, H.H. Hsu**The influence of obliquity in the early Holocene Asian summer monsoon**

Geophys. Res. Lett., 43 (2016), pp. 4524-4530

Wu et al., 2009b

G.X. Wu, Y. Liu, X. Zhu, W. Li, R. Ren, A. Duan, X. Liang**Multi-scale forcing and the formation of subtropical desert and monsoon**

Ann. Geophys. Ger, 27 (2009), pp. 3631-3644

Wu et al., 2012

G.X. Wu, Y.M. Liu, B.W. Dong, X.Y. Liang, A.M. Duan, Q. Bao, J.J. Yu**Revisiting Asian monsoon formation and change associated with Tibetan Plateau forcing: I. Formation**

Clim Dyn, 39 (2012), pp. 1169-1181

Wu and Zhang, 1998

G.X. Wu, Y.S. Zhang**Tibetan plateau forcing and the timing of the monsoon onset over South Asia and the south China sea**

Mon. Weather Rev., 126 (1998), pp. 913-927

Xie et al., 2006

S.P. Xie, H.M. Xu, N.H. Saji, Y.Q. Wang, W.T. Liu**Role of narrow mountains in large-scale organization of Asian monsoon convection**

J. Clim., 19 (2006), pp. 3420-3429

Yanai et al., 1992

M.H. Yanai, C.F. Li, Z.S. Song**Seasonal heating of the Tibetan Plateau and its effects on the evolution of the asian summer monsoon**

J. Meteorol. Soc. Jpn., 70 (1992), pp. 319-351

Yuan et al., 2004

D. Yuan, H. Cheng, R.L. Edwards, C.A. Dykoski, M.J. Kelly, M. Zhang, J.Qing, Y. Lin, Y. Wang, J. Wu, J.A. Dorale, Z. An, Y. Cai**Timing, duration, and transitions of the last interglacial Asian monsoon**

Science, 304 (2004), pp. 575-578